The Libyan Journal of Science
University of Tripoli Vol. 27, No. 02
https://uot.ed.ly/journals/index.php/ljs

Evaluate Fire Radiative Power (FRP) from Oil field emissions over Oil Crescent of Libya, using Satellite techniques of VIIRS-Suomi bands

Dawi Muftah Ageel

Department of Ecology, Faculty of Science, University of Almergib

Corresponding author: dmageel@elmergib.edu.ly

A R T I C L E I N F O

Article history:

Received 28/05/2024

Received in revised form 11/08/2024

Accepted 21/08/2024

A B S T R A C T

Under climate change conditions, gases from oil fires may cause environmental damage proportional to the number of oil fields and their production capacity. Fire Radiant Power (FRP) used as an indicator of the combustion area (emission). The spatial resolution of bands were 370 m per pixel. The results showed high productivity in large fields such as Wahat 3.62 FRP 347.33 BT and Nafora-C 3.24 FRP with 335.46 BT, the weakest field recorded in Intisar-A was 0.6 FRP and 299.21 BT. For a monthly time series, in April highest FRP value recorded, the weak values were recorded in winter and fall months. This study recommends a health survey of workers and residents near those fields, and a field assessment of air pollution for the entire oil crescent is needed.

Keywords: FRP,VIIRS, Satellite, Oil Crescent, Libya.

1. Introduction

Oil associated gas is produced along with crude oil as shown in table(1),in oil reservoirs, either dissolved in the oil or as a gas dome above the oil in the reservoir[1]. Historically, this gas present with crude oil and removed with production waste in the oil extraction industry. Since many of the fields are remote in the prairies and seas, this associated gas was burned to get rid of it and this burned gas called ignition gas[2]. Benefit from the gas in several ways after processing it, by selling it, or using it to generate electricity on site using electric generators or a turbine engine. Also, inject gas into the reservoir to enhance or improve oil extraction or be used as a raw material in petrochemical plants [3]. Russia tops the list of countries that flare the most associated gases, burning 30% of all associated gases flared in the world [4].Flaring of associated gases is controversial because it pollutes the atmosphere, exacerbates global warming, and is a waste of a valuable energy source.

Associated gas is flared in many energy-short countries[5].In the United Kingdom, gas cannot be ignited without government permission and approval to avoid waste and to protect the environment[6].The World Bank estimates that 150 billion cubic meters of natural gas is flared or released into the atmosphere annually. This gas is valued at 30.6 billion US dollars and is equivalent to 25% of the annual American gas consumption or 30% of the European Union's annual gas consumption, and convert it into more useful petroleum liquids through gas liquefaction [7].

Table.1. Natural gas components [8]

Gas	Chemical formula	Volumetric percentage (%)
Methane	CH_4	81
Ethane	C_2H_6	5.5
Propane	C_3H_8	6.6
Butane	C_4H_{10}	4
Pentan	C_5H_{12}	1.4
Nitrogen	N_2	1
Carbon dioxide	CO_2	0.7

A fire of these gases burns violently out of control, and progresses through four different stages: ignition, flame, combustion, and extinction . Fire severity can vary primarily in relation to the moisture content of the combustible material, wind, air temperature, humidity, and slope. The amount of fuel load available is one of the most important variables that affect the behavior and severity of a fire [9]. Gases and aerosols released into the atmosphere during the combustion process have a significant impact on atmospheric chemistry and the regional and international land environment [10]. Most of these emissions occur during the flame and combustion phases. The majority of carbon monoxide, carbon dioxide, and water emissions occur during the flame phase; In the ignition stage, most trace gases and particulate matter are released [11].

Hot spots exist everywhere on the FRP product, implemented by Suomi bands, monitors the total radiative energy of all detectable land hotspots on our planet[12].Industrial gas flares emit radiation signatures with high seasonal and geographic variability. When these events are not controlled, they can have devastating effects on our global atmosphere, and on those living in nearby areas[13].In addition to its primary marine and continental targets, the FRP scale on board of VIIRS satellite, detects and monitors direct threats of any "burning" events over an area of 375 metres. They are usually grouped under the term hotspots.The FRP processor determines the radiative power of any hotspot found on Earth's surfaces. All hotspots were identified and marked within three hours of the VIIRS observation time. The ground temperature about 300 K, and the burning temperature between 75to1200 K [14].The heating flame (FRP) generated by the flammable gas can sometimes heat beyond 1,500 K. Hence, they are generally classified as hotspots. Regardless of its location (earth surface or ocean), its radiative temperature results in a spectral heating signal that can be seen from space. As temperature increases, the peak radiative emission moves towards shorter wavelengths. Thus, fire signals peak in the mid-wave infrared (MWIR), between 3 and 5 µm, while hotter objects may show a higher signal in the short-wave infrared (SWIR), between 1.5 and 2.3 µm [15]. Another common denominator is their enormous impacts on our environment. Fires are an important source of atmospheric trace gases and black carbon (BC) particles, which harm human health and contribute to climate change.The high frequency of fires leads to an increase in the cumulative buildup of carbon concentrations in the atmosphere. The average global fire emissions for the period 1997-2016 are estimated at 2.2 picograms of carbon per year, with significant inter annual variability. Net greenhouse gas emissions from all fires averaged six percent of global fossil fuel CO2 emissions in 2014, with deforestation and tropical peat fires being the most common source [16].The VIIRS 375 m active fire product builds on the legacy of MODIS fire products, using a contextual multispectral algorithm to identify sub pixel fire activity and other thermal anomalies in Level 1 (patch) input data. The algorithm uses all five 375-meter VIIRS channels to detect fires and separate land, water and cloud pixels in the image. Additional 750 m channels complement the available VIIRS multispectral data. These channels are used as input to the primary active fire detection product, which provides continuity to the EOS/MODIS product of 1 km fire and thermal anomalies [17].The aim of this research is to evaluate of FRP size from the targeted fields.and to identify on the residential communities that near from those fields.Also finding the relationship between FRP and brightness temperature.

2. Method and Materials

2.1. Study Site

Study area as shown in Figure(1) located between 30°.85'10"N, 20°43'29" E & 28°39'930"N, 19°.86'93"E,within the desert lands in eastern Libya. Study area covered 41,812 km^2 , included; Jalo, Awjila, Zala and Jakhrah villages, Zelten ,Messlah,Maged and Al-Nafoura as oil fields. Which are vital areas closely linked to oil production, as they are the main source of oil. However, it is part of the country's oil wealth. Satellite images acquired annually for this area show many active fires. However, only a few studies have been conducted on off-gas fires for these oil fields using VIIRSsatellite data.

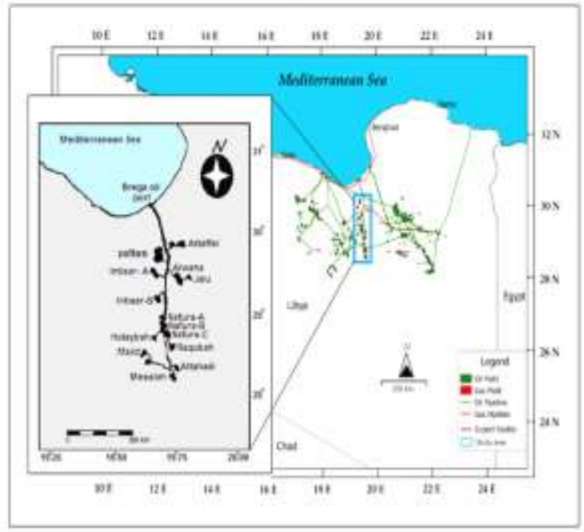

Fig. 1. Study location

As shown in Table (2) [18], data was obtained from the VIIRS sensor aboard the joint NASA/NOAA Suomi National Polar-orbiting Partnership (Suomi, NPP). In this research,hot spots of fire gases was presented in red pixels, each one represent brightness temperature of the fire in kelvin and radiative power of fair in megawatts (MW). Pixel size/dimension is affected by satellite view geometry and curvature of Earth's surface. Consequently, pixel size becomes more distorted with increasing distance from the point immediately below the satellite. The reported coordinate is the center of each pixel's footprint.The fire scars were mapped over a VIIRS images with a spatial resolution of 375 m and an acquisition date of 2023. Fourteen products were downloaded during study area they are selected randomly. The average Fire Radiative Power (FRP) was obtained from the mean value of three VIIRS fire pixels [19]. VIIRS detectors have a fixed angular resolution that results in pixel size detection, Where the scan is identical to the fire location [20]. The fire was further explained while processing a batch of data and deleting overlapping and distorted pixels. The VIIRS 375 m active fire product was described using a fire identification algorithm, which uses pixels as a numerical system of fire coverage areas. The VIIRS sensor on board the Suomi NPP satellite is located in equator orbit.

Table. 2. Attribute fields for NRT VIIRS 375 m active fire data

Attribute	Short Description	Long Description
Latitude	Latitude	Center of nominal 375 m fire pixel
Longitude	Longitude	Center of nominal 375 m fire pixel
Bright_ti4	Brightness -temperature I 4	channel brightness 4-VIIRS I temperature of the fire pixel .measured in Kelvin
Scan	Along Scan pixel size	The algorithm produces approximately 375 m pixels nadir. Scan and track at .reflect actual pixel size
Satellite	Satellite	-N= Suomi National Polar orbiting Partnership (Suomi 20-NPP), 1=NOAA prior to 1-designated JPSS) (launch
FRP	Fire Radiative Power	-FRP depicts the pixel integrated fire radiative .(MW (megawatts power in

2.2. Brightness algorithm

For calculate brightness temperature, Plank law used as follow in equation (1), [21]:

$$I_v = \frac{2\,h\,v^3}{c^2}\,\frac{1}{e^{\frac{hv}{k\,T}} - 1} \qquad (1)$$

Where

I_V is the Brightness Temperature size ,

e is the amount of energy emitted per unit surface area,

T is the temperature of the red body

h is Planck's constant; ***v*** is frequency; c is the speed of light; and

k is the Boltzmann constant.

2.3. FRP account

Fire pixel saturation have fourteen channel in the mid-infrared, and calculated using

VIIRS data by following algorithm (2), [22]:

$$FRP = \frac{A\,\sigma\,(L_{13-}L_{13B}\ )}{\alpha}\,.\,10^{-6} \qquad (2)$$

Where

A is the pixel area which varies as a function of scan angle.

σ is Poltzman constant (5.67×10^{-8} $Wm^{-2}K^{-4}$).

α is a channel-specific constant(VIIRS M13=2.88×10^{-9} Wm).

L_{13} is the M13 channel fire pixel.

L_{13B} is mean background radiances.

2.4. Regression analysis

For clarify relationship between FRP and I_v (brightness temperature), MATLAB program analyzer used the following formula(3),[23],it allows the variable values to be classified into multiple colors. Therefore, it was preferred because it clarifies these values more precisely and eliminates the harsh and divergent values.

$$FRP= 8.3338 \times 10^{-5} \times I_v^3 - 6.11707 \times 10^2 \times I_v^2 + 14.8674x\ I_v - 1150.92 \qquad (3)$$

Where

I_v in kelvin (K), and FRP in mega watt(mw).

3. Results and Discussion

3.1. Detection of FRP distributions

Red pixels used to represent AFP, which expresses the intensity of heat emitted by gases resulting from combustion. Thermal anomalies (Or known as the gastail) that do not express on the combustion intensity were hidden, as it is far from the emission center and would be a false alarm for it. The spatial resolution technique was used daily during the study year (2023).

The VIIRSuomiBand algorithm's output classification - Band-of regional emitted gases reflects the size of the I pixelsn the same day and at those emitted o ‹ approximately the same time. Through Figure(2b) thermally anomalous and spatially isolated pixels were detected and they were classified as ‹FRPpixels due to their presence in an area dominated by oilfiand their ‹ tion was not identified as the location of true rather loca They are therefore included in .detection than false alarm

the final outputFRPpixel array.They are all associated with gase missionsand although they are not located in ‹ urbancenters ‹theyated on the edges of or close to are loc large oil fields and contain similar emission sources.as in Figure2

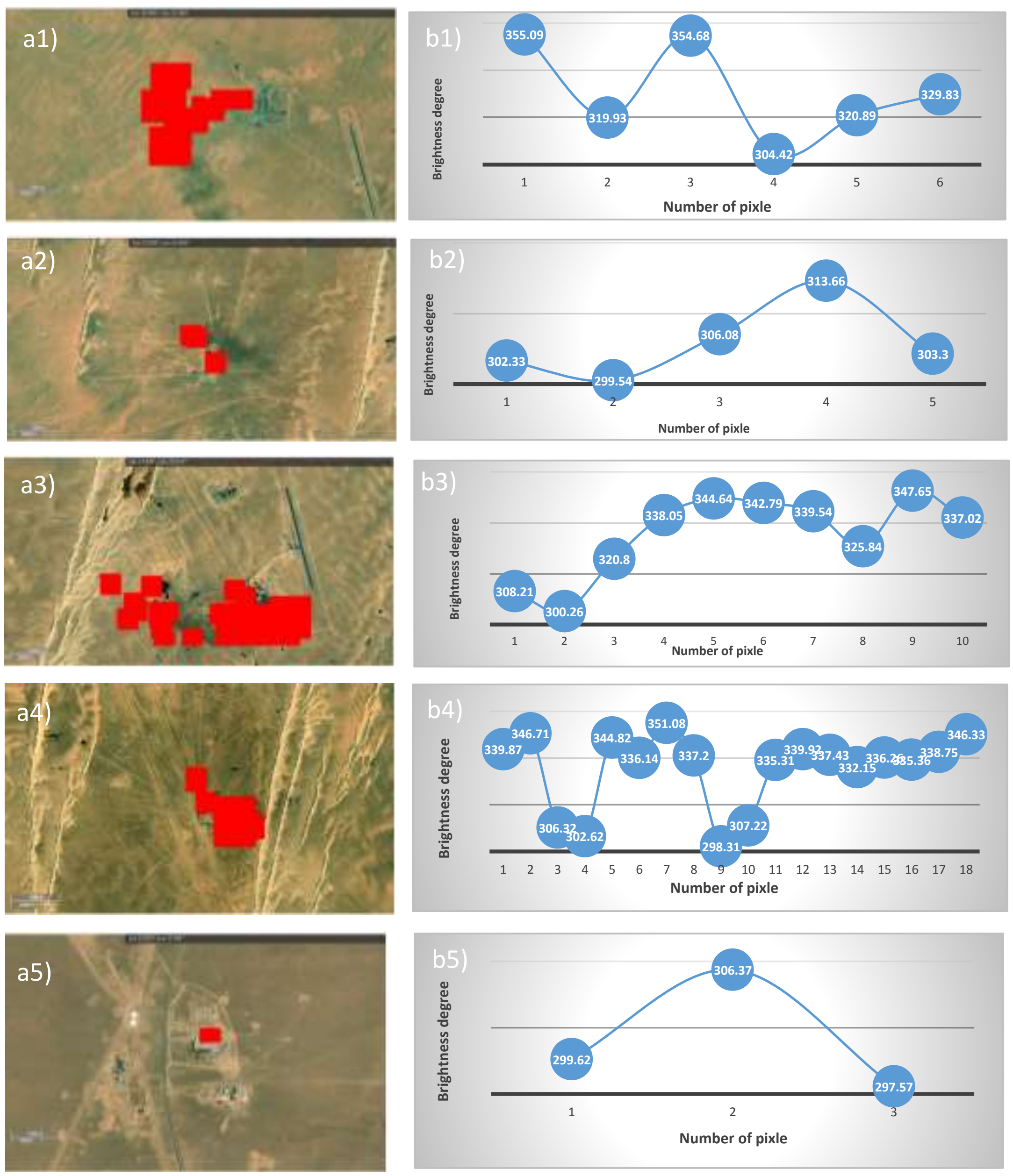

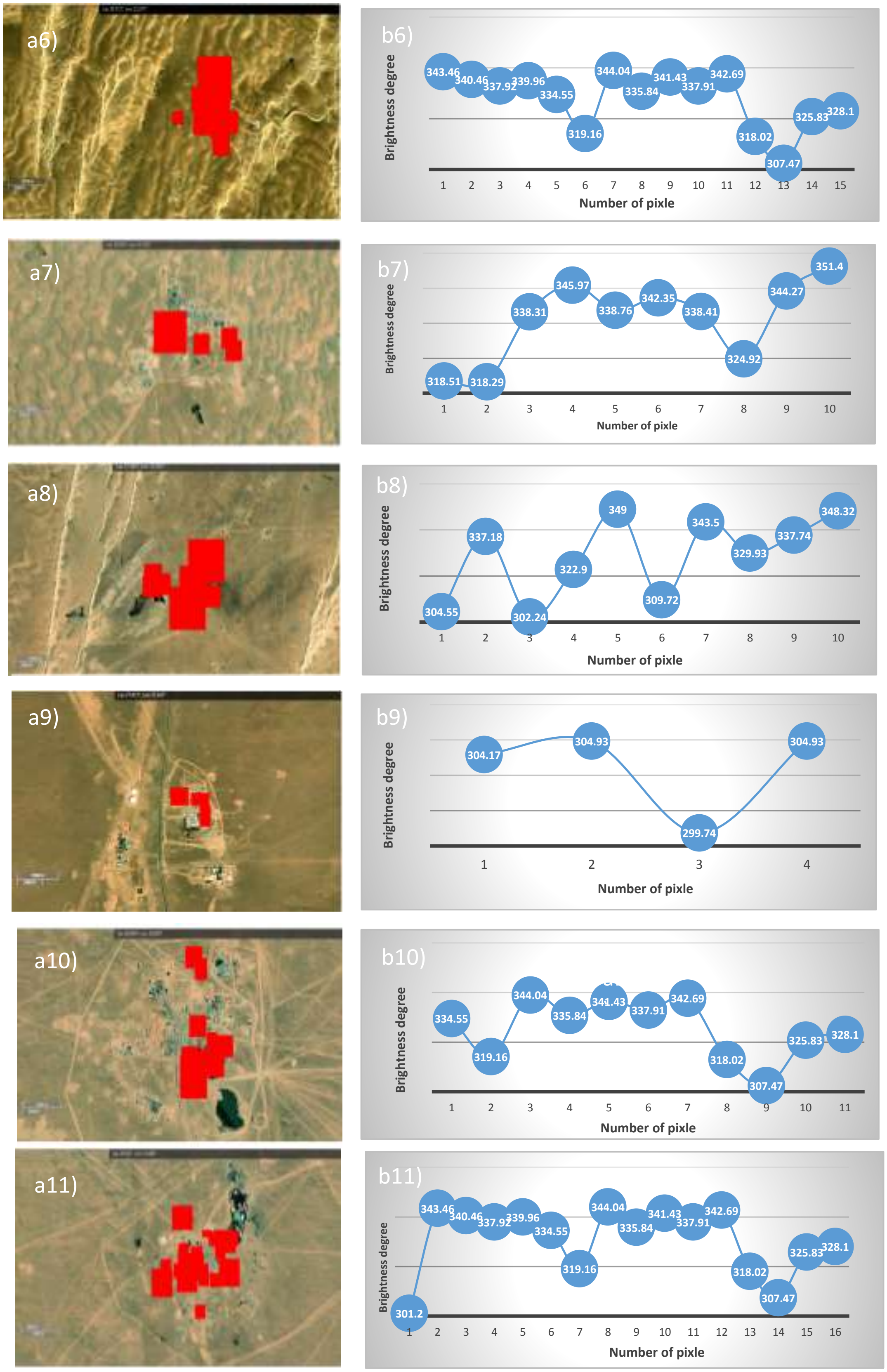
a6)
b6)
Brightness degree
343.46 340.46 337.92 339.96 334.55 319.16 344.04 335.84 341.43 337.91 342.69 318.02 307.47 325.83 328.1
1 2 3 4 5 6 7 8 9 10 11 12 13 14 15
Number of pixle
a7)
b7)
Brightness degree
318.51 318.29 338.31 345.97 338.76 342.35 338.41 324.92 344.27 351.4
1 2 3 4 5 6 7 8 9 10
Number of pixle
a8)
b8)
Brightness degree
304.55 337.18 302.24 322.9 349 309.72 343.5 329.93 337.74 348.32
1 2 3 4 5 6 7 8 9 10
Number of pixle
a9)
b9)
Brightness degree
304.17 304.93 299.74 304.93
1 2 3 4
Number of pixle
a10)
b10)
Brightness degree
334.55 319.16 344.04 335.84 341.43 337.91 342.69 318.02 307.47 325.83 328.1
1 2 3 4 5 6 7 8 9 10 11
Number of pixle
a11)
b11)
Brightness degree
301.2 343.46 340.46 337.92 339.96 334.55 319.16 344.04 335.84 341.43 337.91 342.69 318.02 307.47 325.83 328.1
1 2 3 4 5 6 7 8 9 10 11 12 13 14 15 16
Number of pixle

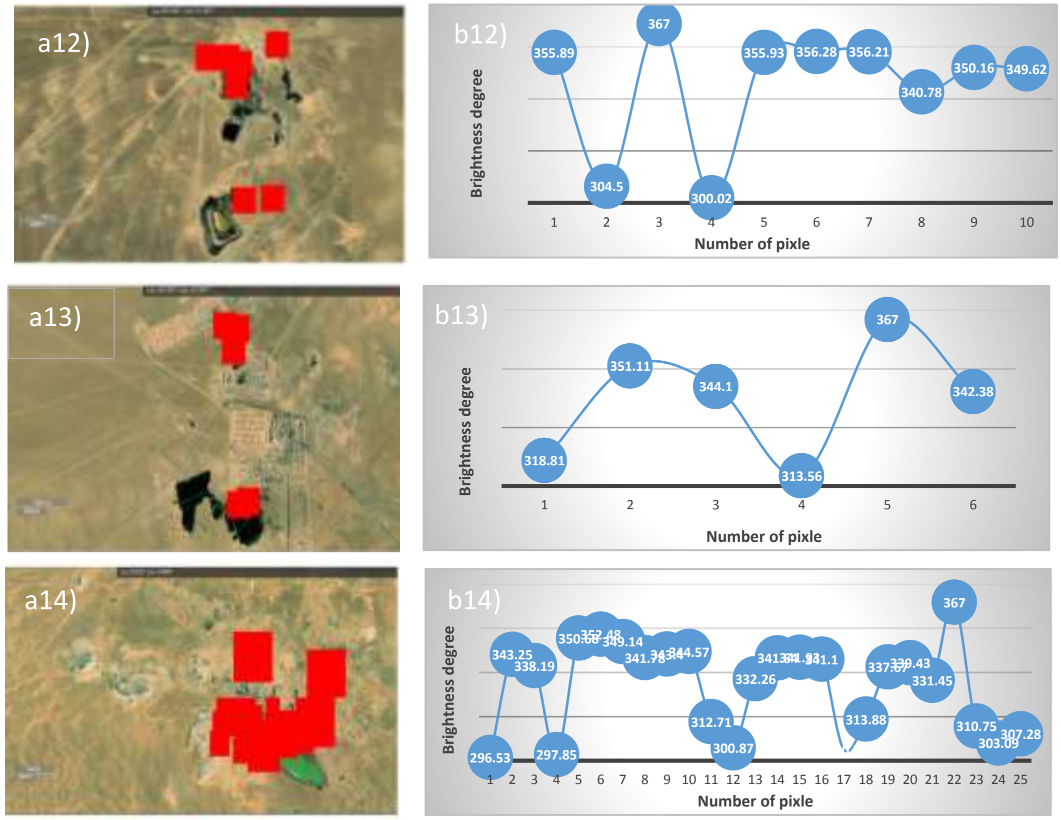

Fig.2. Shows lift column (Fig.2A) represents red channel pixels of gas emissions from oil and gas fields, while into right column (Fig.2B) shown b rightness temperaturerates measuredin Kelvin with pixel numbers

The pixels in red channel to evaluate the brightness degree to each pixel recorded from the spatial data over studyareaA). And In -as shown in Figure 2 (column ، the same figureinThe brightness degree .(B-column) Band-was calculated using the VIIRS Icurvewhere ، the brightness value was 347 within 25pixelswhile the ، minimum degree was 296 within 4 pixels. The pixel colors were displayed in two shades ofredlight red ، and darkred dark red indicate to high emission ، concentrationicate to low emission while light red ind ، concentration. From the obtained data found that 88% appeared in dark red and located in the emissioncenter ، while 22% represented light red and located far from the emission center. Fire Radiation Power (FRP) in Figure variation between 1.5 to 3.5 megawatts showed a (3) (mwduring studywhere ،(2023)) months of year observed that highest level of FRP value started to rise in March until the beginning ofAprilthen started to ، April. In the summer-decrease until midseasonFRP ، were high with 23% of missing data due to strong value .southeasterly winds or scattered cloudsin fallseason, A noticeable decrease was recorded , from 0.1 to 0.3 mw, with missing data reaching to 77%. winter season f some obstacles to data were very weak because o capturing VIIRS images such as dusthaze cloud ،shine ، and dispersion of gas emissions by westerly winds or dust storms. Only in early January there was little data not exceeding 0.5mw ،and 2.25 mw value recorded in last January as evidence on disappearance of the previously mentioned barriers.

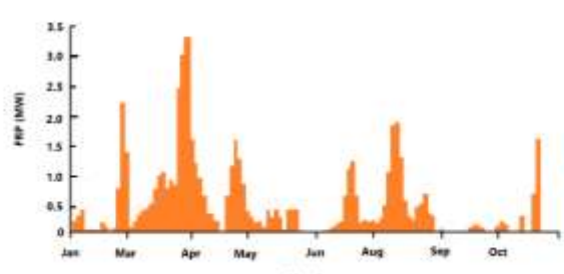

Fig.3. Daily data of FRP rates during study year

In the following table(3), shown fourteen oil fields was targeted in this study,with attribute fields of VIIRS Soumi bands.where observed that Wahah field emissions was higher value of FRP, then Nafura-C and Zaltan fields respectively, because of they are biggest fields from the rest of fields. Higher FRP rate observed in Wahah field was 3.47 mw and lowest FRP rate was 0.6 mw in Intisar-A field, this meaning that size of field and emission time with along scan or along track were factors linked with each other.

In Figure(4), showed histogram from highest to lowest emission of study wells respectively, and found convergence between high values of Wahah, Nafura-C, Zaltan,and Majid fields, because of high in brightness temperature,and FRP, but there were low values from along scan or along track to same fields. Also showed in August was prevalent as the highest emissions from these fields, and weak in October. Highest brightness temperature observed in Jalu field with FRP value is weak; this mean there is positive relationship between FRP emissions and brightness temperature.

Table.3. Study fields and their products from FRP

No.	Location	Latitude	Longitude	Brightness Temperature	Along Scan	Along Track	Month	FRP
1	Wahat	27.98428	22.32694	347.33	1.18	1.08	3-2023	3.62
2	Intisar A	27.98593	19.90727	299.21	0.56	0.43	10-2023	0.6
3	Intisar B	28.05612	19.91298	315.67	0.57	0.63	8-2023	1.74
4	Zaltan	28.05612	19.91298	328.24	0.44	0.75	4-2023	3.09
5	Messlah	28.05612	19.91298	309.21	0.57	0.44	8-2023	1.78
6	Attiffel	28.91448	19.77789	299.85	0.65	0.73	8-2023	1.29
7	Majid	28.9097	19.77543	312.77	0.41	0.37	3-2023	2.98
8	Jalu	28.88598	19.80692	311.74	0.72	0.76	8-2023	1.06
9	Nafura-A	28.10138	19.25169	306.41	0.44	0.46	8-2023	1.01
10	Nafura-B	28.90403	20.95813	304.72	0.51	0.41	8-2023	2.32
11	Nafura-C	28.90633	20.95741	335.46	0.39	0.44	4-2023	3.24
12	Raqubah	28.90701	20.95312	341.35	0.64	0.54	3-2023	2.02
13	Attahadi	28.91092	20.96698	302.85	0.63	0.54	4-2023	1.54
14	Hutaybah	28.8996	20.96278	306.15	0.51	0.41	6-2023	0.91

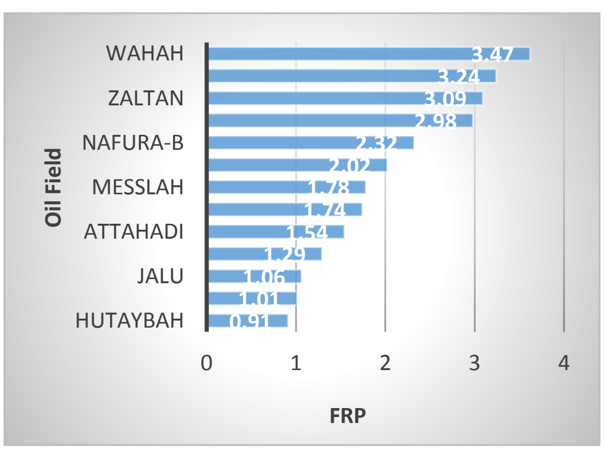

Fig.4. Histogram shown oil and gas wells with their FRP emissions

3.2 Verification from Residential environment close to fields

Three residential communities were identified at the studysitewhich were close to gas emissions from the studyfieldsand are often expected to be more vulnerable to these hazardous emissions. Many of these communities are concentrated in three regions with similar demographiccharacteristics-such as: Jalu, Al Wahat, Mizdah, and Jakherah. It is exposed to the contaminated groundwater and air danger of .pollutionTheylives approximately one kilometer from oil and gas wells. Forexample ،Jalu and Gekera and AlWahat are 20 km away from Al Wahat field and ، Mrada. is 50 km away from Zalten field. Population statistics for the areas near the study fields were as follows: in Awjila village were 8,515 people according to the 2006 census, in Jalu village 7,963 people according to the 2010 census, in Jakhra village arrive to 4,117 people according to the 2006 census, and in Marada village were 2,229 people according to the 2006 census. They live within 1 to 15 miles of active oil fields. Figure (5) shows residential communities near these -birth-fields are more at risk of prematur birth, low weight babies than normal, acute respiratory diseases, and cancer[24]. Living near oil wells is associated with decreased lung function andwheezing and in some ، casesdamage to the respiratory system rivals that from ، daily exposure to secondhand smoke or living next to a highwayaccording to a recent study published in the ، Journal of Environmental Research [25].Environmental advocacy groups have urged the . foot buffer zone, between fossil fuel -a 2,500 creation of operations, homes and schools[26].

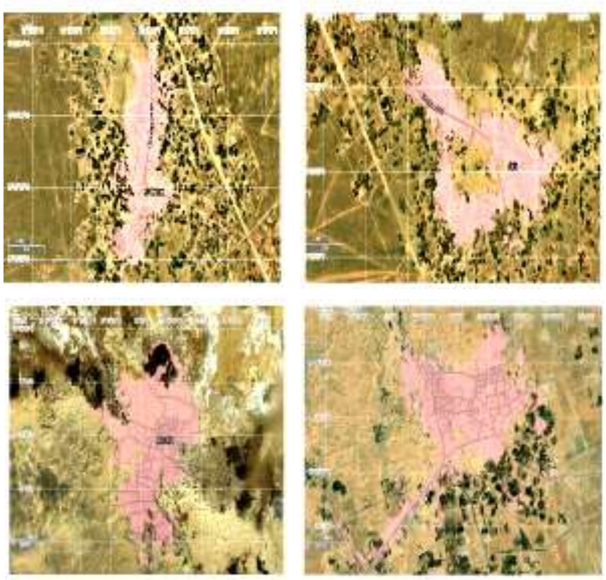

Fig.5. Habitat close to emission sources

The relationship between brightness temperature from VIIRS-Suomi band data (vertical axis) and FRP for same fire pixel from VIIRS-Suomi band fire product (Horizontal axis), colors in dots refers to correlation even small fires. In Figure (6) shown RGB (red,green and blue) color values, where red color represents strong relation values between bright temperature and Fire Radiative Power, with range 1.0 to 2.5 megawatts , and 300 to 330 kelvin. Yellow, green and cyan colors represents duplicates dots between bright temperature (T_b) and FRP values, with range 331 -335 kelvin and 2.60 to 2.75 megawatts. The relationship between two variables started to change in blue color with high values of each of them, regression line gives a clear negative relationship, but it is weak and not affect on strong positive relation. For range from 2.76 to 3.5 mw with 340 t0 350 (k), they are represents dispersion values (negative relationship) and the positive relationship decrease.

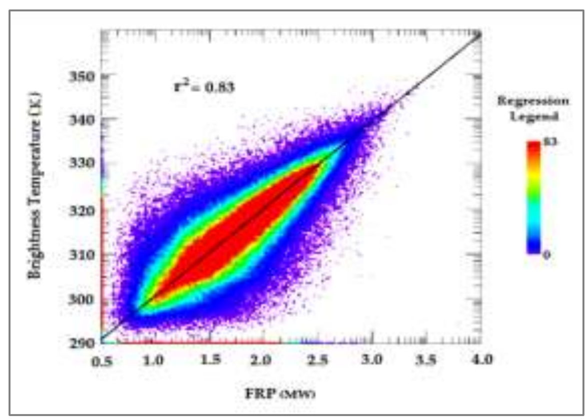

Fig.6. Numerical relation between Brightness temperature (K) and FRP data

4. Conclusion

Fire radiant power (FRP) with the 375-meter VIIRS I-Band data were very low FRP, which represented false alarms. A small number of these alarms were verified using high spatial resolution images before and after firing, which showed that burned areas. VIIRS data had significant advantages,it detected active fires with a minimum FRP of less than 1 mw. From analyzed data showed that FRP values was not high (up to 5mw)

, which indicates to wavelengths that used in distinguish FRP in red color. Also these findings highlight the importance of a strong approach to protecting mmunities on the front lines from the harmful impacts co associated with oil and gas production. For this reason, environmental protection professionals must rely on robust and comprehensive methods that include basic ons even in provisions such as frequent leak inspecti smaller wells.And to have strict air pollution rules that would protect those communitiesfromoil and gas ‹operations thisrequire inspections at all well sites and prohibit burning of the oil randomly.

5. References

1. .(Energy.(2019 of US.,Department Natural Gas Flaring and Venting: State and Federal Regulatory Overview, Trends, and Impacts,72.
2. Tennyson,.M.E.(2005).Growth History of Oil Reserves during the Twentieth Century.Chapter H of Geologic, Engineering, and Assessment Studies serve Growth,.120of Re p.
3. Hannah Ritchie and Max Roser .(2020). Energy. Published online at OurWorldInData.org. .https://ourworldindata.org/energy :Retrieved from
4. s Roland,. T, H. (2010). Associated Petroleum Ga utilization . FNI -in Russia: Reasons for Non Report 13. Lysaker: Fridtjof Nansen Institute,53 .
5. Hessler,.A.M.(2011).Earth Earliest Climate. Nature Education Knowledge.J. 3(10):24-56.
6. EANLGG.(2023).Guidance on Landfill Gas Flaring.The Environment Agency's National Landfill Gas.,56.
7. The World Bank.(2022). Global Gas Flaring Tracker.Global Flaring and Methane Reduction Partnership,. Report,28April,37p.
8. Jan Siazik & Milano Malcho.2017.Accumulation of Primary Energy Into Natural Gas Hydrates.Procedia Engineering Journal.,192:782-787
9. Whelan, R.J.(2015). The ecology of fire. UK: Cambridge UniversityPress, 360p .
10. Longo, K.M.; Freitas, S.R.; Andrea, M.O.;Yokelson, R.; Artaxo, P.(2021). Biomass burning in Amazonia,AGU Publishing,32.
11. .M.O ‹Andrea(2019)Biomass burning: Its history, . tion and its impact on -use and distribu :nI .mate-environmental quality and global cli spheric, -Global biomass burning: Atmo .LEVINE, J :c Implications.CambridgeClimatic and Biospheri .Press MIY2(3):5-21.
12. -pixel-David P,.Charles I,Edward. J.(2013).A sub based calculation of fire radiative power from observations.Remote Sensing of MODIS ‹Environment2(5):262-279.
13. Freitas, SR.; Longo, K. M.; Sil Vadias, M.A.(2015). Emissões de queimadas em ca do Sul. Estudos ecossistemasda Améri ‹Avançados.J5(3):167-185.
14. Sullivan, G. M., & Artino Jr., H. R.(2013). Analyzing and Interpreting Data from Likert-Type Scales. The Journal of Graduate Medical Education, 3(10): 532-541.
15. Toreyin,. B.U.(2018). Fire Detection Algorithms Using Multimodal Signal and Image Analysis, PhD thesis Bilkent University, Department of Electrical and Electronics Engineering, Ankara-Turkey.
16. Lan, X., B. D. Hall, G. Dutton, J. Mühle, J. W. Elkins, and I. J. Vimont.(2022). Long-lived greenhouses gases in State of the Climate in 2021, Chapter 2: Global Climate,J. Bulletin of the American Meteorological Society, 103 (8):81-104.
17. Maier, S.W.; Russel,S, J.; Edwards,A.C.;Yates, C.(2011). Sensitivity of the MODIS fire detection algorithm (MOD14) in the savanna region of the Northern Territory, Australia. Journal of Photogrammetry and Remote Sensing, . 6(2):119-127.

18. VIIRS active fire files,NASA(2024).Published on linefrom:https://www.earthdata.nasa.gov/learn/find-data/near-real-time/firms/viirs-i-band-375-m-active-fire-data.
19. Fidelis, A.; Delgado-C, D.; Blanco, C.C.(2010). Fire intensity and severity in Brazilian campos grasslands. Interciencia-Caracas.J,3(10)**:** 739-745.
20. Pereira, G; Cardozo, F.S.; & Silva, F.B.(2012). Determination and modeling the consumption rate of burned biomass . Revista Brasileira de Meteorologia.Journal,23(5): 69-82.
21. Siegel,R.Howell,J.(2002). Thermal radiation heat transfer, Fouth edtion,Taylor & Francis publishes,835p.
22. Wooster, M.J.; Roberts, G.; Perry, W.(2005). Retrieval of biomass combustion rates and totals from Fire Radiative Power(FRP) observations: Journal of Geophysical Research, 3(7):223-241.
23. Giglio, L., and Justice,C.O.(2003). Effect of wavelength selection on characterisation of fire size and temperature, Int. J. Remote Sens., 2(4):515–520.
24. Chang, H. H., Reich, B. J. & Miranda, M. L.(2021). A spatial time-to-event approach for estimating associations between air pollution and preterm birth. J. R. Stat. Soc. Ser, 6(2):167–179.
25. Czolowski ED, Santoro RL, Srebotnjak T, Shonkoff SBC.(2017). Toward Consistent Methodology to Quantify Populations in Proximity to Oil and Gas Development: A National Spatial Analysis and Review. Environmental health perspectives ;125.
26. Ferrar KJ, Kriesky J, Christen,.CL.(2013). Assessment and longitudinal analysis of health impacts and stressors perceived to result from unconventional shale gas development in the Marcellus Shale region. International Journal of Occupational and Environmental Health ;9(3):104–112.